Geometries and Electronic Structures of Group 10 and 11 Metal Carbonyl Cations, $[M(CO)_n]^{x+}$ ($M^{x+} = Ni^{2+}, Pd^{2+}, Pt^{2+}, Cu^+, Ag^+, Au^+$; $n = 1-4$)

Koichi Mogi,*,† Yoshiko Sakai,† Takaaki Sonoda,† Qiang Xu,‡ and Yoshie Souma‡

Department of Molecular and Material Science, Kyushu University, 6-1 Kasuga Park, Kasuga, Hukuoka, 816-8580, Japan, and National Institute of Advanced Industrial Science and Technology, AIST, 1-8-31 Midorigaoka, Ikeda, Osaka, 563-8577, Japan

Received: September 11, 2002

The geometry and electronic structure of group 10 and 11 metal carbonyl cations, $[M(CO)_n]^{x+}$ ($M^{x+} = Ni^{2+}$, Pd^{2+}, Pt^{2+}, Cu^+, Ag^+, Au^+; $n = 1-4$), were examined by the hybrid density functional method (B3LYP) and the coupled cluster method (CCSD(T)). For group 10 metals, monocarbonyl cations have $C_{\infty v}$ structures, dicarbonyl cations have $D_{\infty h}$ and C_{2v} structures, and tri- and tetracarbonyl cations have C_{2v} and D_{4h} structures, respectively. Group 11 metal carbonyl cations have $C_{\infty v}$, $D_{\infty h}$, D_{3h}, and T_d structures for mono-, di-, tri-, and tetracarbonyls, respectively. The $(CO)_{n-1}M^{x+}-CO$ dissociation energies D_0 (CO) of group 10 metal carbonyl cations are significantly larger than those of group 11 metal carbonyl cations. Group 10 metal tetracarbonyl cations are still stable, while for group 11 metals, D_0 (CO) is significantly reduced in going from dicarbonyls to tri- and tetracarbonyls. The vibrational frequencies ν(CO) are higher by 110−165 cm^{-1} for group 10 metal complexes and by 45−115 cm^{-1} for group 11 metal complexes than that for free CO (2143 cm^{-1}).

1. Introduction

The metal carbonyls are well-studied and understood.[1] For neutral metal carbonyls, such as $Ni(CO)_4$, $Fe(CO)_5$, and $Cr(CO)_6$, the vibrational frequencies, ν(CO), are considerably lower than the value for free CO (2143 cm^{-1}). The carbonyl group acts as an electron acceptor from *d*-block metals though π back-donation. Many industrial processes employ metal carbonyls as catalysts for hydroformylation and in the Fischer−Tropsch synthesis of acetic acid.

Copper carbonyl cations $[Cu(CO)_x]^+$ ($x = 1, 2$), the first metal carbonyl cation generated, were studied by Souma in the 1970s in acidic solution.[2] Strauss[3] succeeded in isolating and characterizing silver carbonyl cations crystallographically; $[Ag(CO)_n]^+$ ($n = 1, 2$) is neutralized by weakly coordinating counteranions. Willner and Aubke[4] synthesized $[Au(CO)_2]^+$ in superacids, Sb_2F_{11}. For group 11 metals, dicarbonyl cations are most stable in acidic solution,[2] and tri- and tetracarbonyl cations can be observed under high CO pressure in acidic solution[5] or isolated using a very weak coordinating counteranion, $[Cu(CO)_4(1-Bn-CB_{11}F_{11})]$.[6] Strauss called these metal carbonyl cations "nonclassical metal carbonyls", since they have higher vibrational frequencies than free CO (2143 cm^{-1}).[7] Metal carbonyl cations are expected to have highly catalytic activity in the Koch reaction,[8] a well-known acid-catalyzed carbonylation. In strong acids, the dicarbonyl cations of group 11 metals $[M(CO)_2]^+$ (M = Cu, Ag, and Au) catalyze the carbonylation of olefins at room temperature and atmospheric pressure to produce tert-alkanoic acids in high yield.[9] This improved process is used by Idemitsu Petrochemical Co. Ltd.[10]

Some ab initio studies[11,12] on group 11 metal carbonyl cations have been reported in recent years, where the molecular geometries, M−CO bond energies, and higher C−O vibrational frequencies ν(CO) than free CO value have been discussed. For typical neutral metal carbonyls, it is understood that the M−CO bond is formed by σ donation from CO(5σ) to the metal and π back-donation from the metal to the empty CO($2\pi^*$). Because the π back-donation weakens the C−O bond, neutral metal carbonyls have lower ν(CO)s than free CO. For metal carbonyl cations, however, the π back-donation is much reduced as compared to that for neutral metal carbonyls, and the electrostatic effects predominate to form M−CO bonds and strengthen the C−O bonds. The electrostatic effects on the high ν(CO)s in metal carbonyl cations were discussed in detail by Goldman et al.[13] and Lupinetti et al.[14]

For group 10 metals, mono-, di-, and tetracarbonyl cations $[M(CO)_n]^{2+}$ ($M^{2+} = Ni^{2+}$, Pd^{2+}, Pt^{2+}; $n = 1, 2, 4$) have been observed experimentally,[15] while the tricarbonyl cation has not yet been observed. Monocarbonyl cations have a linear form,[19a] dicarbonyl cations have bent[19b,c,f] and linear[19b,e] forms, and tetracarbonyl cations have a square planar form.[19d] Group 10 metal carbonyl cations exist as stable crystals in superacids, i.e., $[Pd(CO)_4](Sb_2F_{11})_2$ and $[Pt(CO)_4](Sb_2F_{11})_2$. All group 10 metal carbonyls also have shorter C−O bonds and a higher ν(CO) than free CO and are classified as nonclassical metal carbonyl cations. Binuclear metal−metal carbonyl cations have also been found for group 10 metals, such as the dicarbonyl cation $[Pd_2(CO)_2]^{2+}$ and the hexacarbonyl cation $[Pt_2(CO)_6]^{2+}$.[16] $[Pd_2(CO)_2]^{2+}$ has a CO-bridged form, while three carbonyls are bound to each metal terminally in $[Pt_2(CO)_6]^{2+}$. We[17] have studied the electronic structures of these group 10 binuclear metal−metal complexes theoretically using the B3LYP and CCSD(T) methods. $[M_2(CO)_2]^{2+}$ and $[M_2(CO)_6]^{2+}$ ($M^+ = Ni^+$, Pd^+, Pt^+) are classified as classical and nonclassical metal carbonyl cations, respectively, because ν(CO) is lower in $[M_2(CO)_2]^{2+}$ and higher in $[M_2(CO)_6]^{2+}$ than that of free CO.

In this paper, we study the electronic structures of $[M(CO)_n]^{x+}$ ($M^{x+} = Ni^{2+}$, Pd^{2+}, Pt^{2+}, Cu^+, Ag^+, Au^+; $n = 1-4$). All of

* To whom correspondence should be addressed. Fax: +81-92-583-7459. E-mail: mogi@mm.kyushu-u.ac.jp.
† Kyushu University.
‡ National Institute of Advanced Industrial Science and Technology.

10.1021/jp0220534 CCC: $25.00
Published on Web 04/19/2003

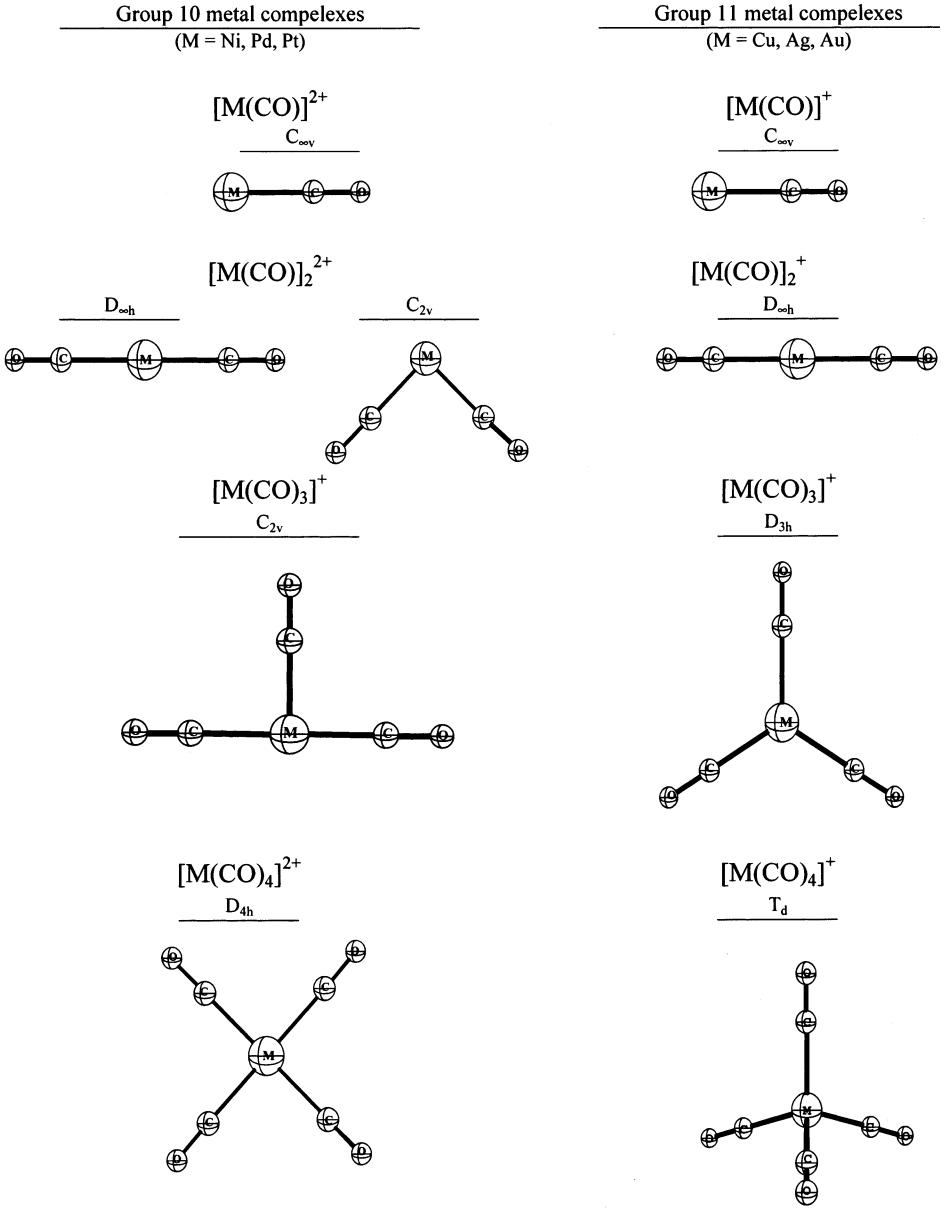

Figure 1. Molecular geometries of group 10 $[M(CO)_n]^{2+}$ (M = Ni, Pd, Pt; $n = 1-4$) and 11 $[M(CO)_n]^{+}$ (M = Cu, Ag, Au; $n = 1-4$) metal carbonyl cations.

these group 10 and 11 metal carbonyl cations are classified as nonclassical metal carbonyl cations, although the conformation and stabilization of group 10 and 11 metal carbonyl cations differ. Although group 11 metal carbonyl cations have been well-studied,[11−16] we included them in this paper because the same quality calculations are required to discuss the differences between the group 10 and the group 11 carbonyl cations.

2. Method of Calculation

All of the optimizations were carried out using the hybrid density functional theory composed using the Becke three-parametrized correlation functional[18] and the Lee−Yang−Parr exchange correlation functional[19] (B3LYP). At the optimized geometries, single point energy calculations were also done to estimate the dissociation energy for the loss of one carbonyl for each $[M(CO)_n]^+$ by the coupled cluster method, including single, double, and triple excitations (CCSD(T)).[20] The effective core potentials and valence basis sets (4211/4211/311) for Ni, Pd, Cu, and Ag and (4111/4111/311) for Pt and Au of Stevens, Basch, and Krauss[21] were used for the calculations. Dunning's correlation consistent basis sets of triple-ζ type cc-pVTZ[22] were used for carbonyls. The optimized free CO bond length by B3LYP (1.126 Å) was in good agreement with experimental data (1.127 Å). For vibrational analysis, the C−O frequencies are multiplied by 0.9692, which is the ratio of the experimental value (2143 cm^{-1}) to the B3LYP (2211 cm^{-1}) value of free CO. Dargel et al.[23] pointed out the significance of the basis set superposition error (BSSE) for the dissociation energy of $[Au(CO)]^+$. The corrections of BSSE and zero-point vibrational energies (ZPE) were done for the dissociation energies $(CO)_{n-1}M^{x+}-CO$. Mulliken population analysis was used to estimate the amounts of σ donation and π back-donation for each $[M(CO)_n]^{x+}$. All of the calculations were performed using the program GAUSSIAN-98.[24]

3. Results and Discussion

A. Molecular Geometries. The optimized geometries of all metal carbonyl cations $[M(CO)_n]^{x+}$ ($M^{x+} = Ni^{2+}$, Pd^{2+}, Pt^{2+}, Cu^+, Ag^+, Au^+; $n = 1-4$) are shown in Figure 1. For group 10 metals, monocarbonyl cations have a $C_{\infty v}$ structure in the

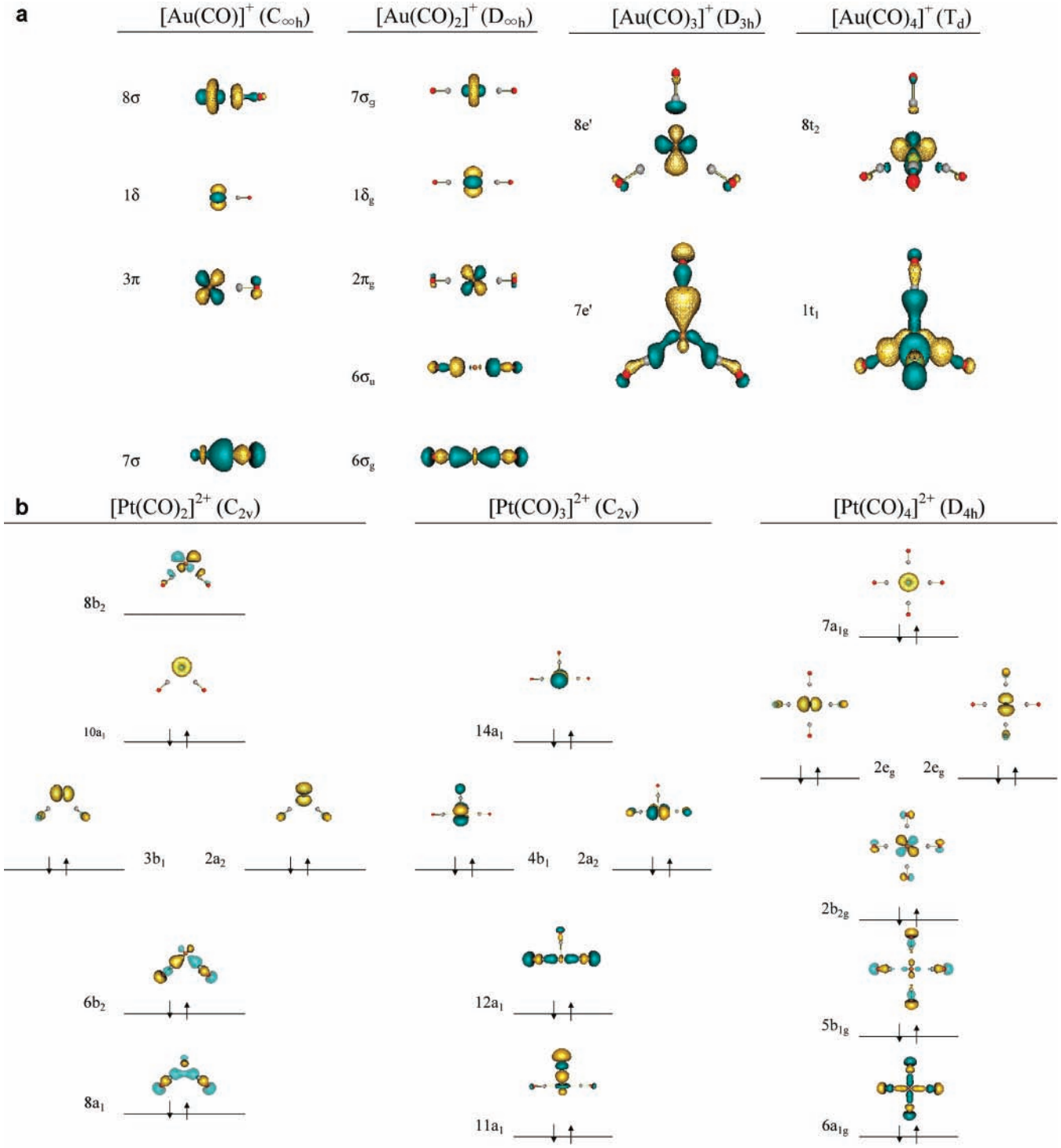

Figure 2. (a) Molecular orbital diagrams of gold carbonyl cations, $[Au(CO)]^+$ ($C_{\infty v}$), $[Au(CO)_2]^+$ ($D_{\infty h}$), $[Au(CO)_3]^+$ (D_{3h}), and $[Au(CO)_4]^+$ (T_d). (b) Molecular orbital diagrams of platinum carbonyl cations, bent $[Pt(CO)_2]^{2+}$ (C_{2v}), T-shaped $[Pt(CO)_3]^{2+}$ (C_{2v}), and $[Pt(CO)_4]^{2+}$ (D_{4h}), where the diagrams of mono- and di(in $D_{\infty h}$) carbonyl cations are not shown because they are nearly the same as those of gold complexes in panel a.

$^1\Sigma^+$ state, dicarbonyl cations have two stable structures of $D_{\infty h}$ and C_{2v} in the $^1\Sigma_g^+$ and $^1A_1$ states, respectively, and tri- and tetracarbonyl cations have a T-shaped (C_{2v}) structure in $^1A_1$ and a D_{4h} structure in $^1A_{1g}$, respectively. In addition, a tricarbonyl cation of D_{3h} structure in $^3A_1'$ was found for M = Ni. For group 11 metals, mono-, di-, tri-, and tetracarbonyl cations have $C_{\infty v}$, $D_{\infty h}$, D_{3h}, and T_d structures in the $^1\Sigma^+$, $^1\Sigma_g^+$, $^1A_1'$, and $^1A_1$ states, respectively. The difference in the geometrical structures between group 10 and group 11 metal carbonyl cations comes essentially from the fact that the number of valence electrons of group 10 complexes is two less than in the corresponding group 11 complexes.

We will discuss the structural difference between group 10 and group 11 metal carbonyl cations with reference to the electronic configurations and molecular orbital diagrams. Figure 2 illustrates the molecular orbitals of (a) gold complexes $[Au(CO)_n]^+$ ($n = 1-4$) and (b) the di- (in C_{2v}), tri-, and tetracarbonyl platinum complexes, $[Pt(CO)_n]^+$ ($n = 2-4$), as examples. The diagrams for mono- and di- (in $D_{\infty h}$) carbonyl platinum complexes are not shown, because they are nearly the

same as those of gold complexes in Figure 2a. The other metal complexes have essentially the same orbital characters for the corresponding complexes.

The electronic configurations of monocarbonyl cations are as follows:

$$[M(CO)]^{2+}\,[C_{\infty v}]:\ \ldots (7\sigma)^2\,(3\pi)^4\,(1\delta)^4 \qquad (M = \text{group 10})$$

$$[M(CO)]^{+}\,[C_{\infty v}]:\ \ldots (7\sigma)^2\,(3\pi)^4\,(1\delta)^4\,(8\sigma)^2 \qquad (M = \text{group 11})$$

where the 7σ and 3π orbitals are involved in σ donation and π back-donation, respectively (Figure 2a). The 8σ orbital is an M−CO antibonding orbital. There is no M−CO interaction in the degenerate 1δ orbitals because of their orbital symmetry. The σ donation and reduced π back-donation contribute to form the M−CO bonds of all metal monocarbonyl cations, while the M−CO bonds of group 11 metal monocarbonyl cations are weakened by the additional 8σ antibonding orbital.

For the dicarbonyl cations, bent[19b,c,f] and linear[19b,e] structures have been found experimentally for group 10 metals, and linear structures[3,4] have been found for group 11 metals. The optimized structures shown in Figure 1 are in accord with the experimental ones. The electronic configurations of linear dicarbonyl cations are as follows:

$$[M(CO)_2]^{2+}\,[D_{\infty h}]:\ \ldots (6\sigma_g)^2\,(6\sigma_u)^2\,(2\pi_g)^4\,(1\delta_g)^4 \qquad (M = \text{group 10})$$

$$[M(CO)_2]^{+}\,[D_{\infty h}]:\ \ldots (6\sigma_g)^2\,(6\sigma_u)^2\,(2\pi_g)^4\,(1\delta_g)^4\,(7\sigma_g)^2 \qquad (M = \text{group 11})$$

The σ donation and π back-donation arise in the $6\sigma_g$ and $2\pi_g$ orbitals, respectively. The $6\sigma_u$ orbital is nearly nonbonding between M−CO. For group 11 metal complexes, the $7\sigma_g$ orbital is localized on the metal in linear dicarbonyl cations, while the 8σ orbital of monocarbonyl cations is a rather strong antibonding orbital as shown in Figure 2a. This could be a reason that dicarbonyl cations are more stable than monocarbonyl cations for group 11 metals.

The group 10 metal dicarbonyl cations in bent structure are more stable than the linear ones. The electronic configuration of bent dicarbonyl cations is as follows:

$$[M(CO)_2]^{2+}\,[C_{2v}]:\ \ldots (8a_1)^2\,(6b_2)^2\,(9a_1)^2\,(7b_2)^2\,(3b_1)^2\,(2a_2)^2\,(10a_1)^2 \qquad (M = \text{group 10})$$

Both the $8a_1$ and the $6b_2$ orbitals are involved in σ donation (Figure 2b). The $3b_1$ and $2a_2$ orbitals are involved in weak π back-donations. There are no M−CO interactions in the $9a_1$, $7b_2$ (not shown in the figure), and $10a_1$ orbitals. As will be shown later, σ donation for bent dicarbonyl cations is larger than that for linear ones, because there are two orbitals involved in the σ donation in the bent form, while only one orbital is involved in the linear ones. The $8b_2$ orbital for the bent $[M(CO)_2]^{2+}$ is the lowest unoccupied molecular orbital (LUMO; see Figure 2b) for group 10 metals, in which M−CO is antibonding. For group 11 metals, this antibonding orbital should be the highest occupied molecular orbital (HOMO). This is a reason that the bent structure does not exist for group 11 metal dicarbonyl cations.

Although group 10 metal tricarbonyl cations have not yet been observed experimentally, we found a stable T-shaped (C_{2v}) structure for all group 10 metals. A planar (D_{3h}) structure was found for group 11 metal carbonyl cations, which is consistent with the experiments.[3] Their electronic configurations are as follows:

$$[M(CO)_3]^{2+}\,[C_{2v}]:\ \ldots (11a_1)^2\,(12a_1)^2\,\ldots (9b_2)^2\,(2a_2)^2\,(4b_1)^2\,(14a_1)^2 \qquad (M = \text{group 10})$$

$$[M(CO)_3]^{+}\,[D_{3h}]:\ \ldots (7e')^4\,(2e'')^4\,(7a_1)^2\,(8e')^4 \qquad (M = \text{group 11})$$

For group 10 metals carbonyl cations, the $11a_1$ and $12a_1$ orbitals are involved in σ donation, and the $2a_2$ and $4b_1$ orbitals are involved in π back-donations (Figure 2b). For group 11 metals carbonyl cations, the $2e''$ and $7a_1$ orbitals do not contribute to the M−CO bonds. As shown in Figure 2a, the $7e'$ orbitals are involved in σ donation. The $8e'$ orbitals are little involved in π back-donations to two carbonyls, while there is a strong antibondimg interaction with the other carbonyl. Thus, the $8e'$ orbitals may weaken the M−C bonds. We also examined the D_{3h} structure in the $^3A_1'$ state for group 10 metal complexes and found a stable $[Ni(CO)_3]^{2+}$ (no imaginary mode was found), whose energy was higher by 8.2 kcal/mol than the one in the T-shaped structure. However, $[Pd(CO)_3]^{2+}$ and $[Pt(CO)_3]^{2+}$ in the D_{3h} structure do not exist and were only found in the dissociations pathway to the dicarbonyl cations.

Group 10 metal tetracarbonyl cations have a planar (D_{4h}) structure, which is made by adding a CO to the T-shaped tricarbonyl cations. Differently from the group 10 metals, group 11 metal tetracarbonyl cations have a tetrahedral (T_d) structure. The square planar[19d] and tetrahedral[3] structures have been observed experimentally for group 10 and group 11 metals, respectively. The electronic configurations of tetracarbonyl cations are as follows:

$$[M(CO)_4]^{2+}\,[D_{4h}]:\ \ldots (6a_{1g})^2\,(5b_{1g})^2\,\ldots (2b_{2g})^2\,(2e_g)^4\,(7a_{1g})^2 \qquad (M = \text{group 10})$$

$$[M(CO)_4]^{+}\,[T_d]:\ \ldots (7t_2)^6\,(1t_1)^6\,(2e)^4\,(8t_2)^6 \qquad (M = \text{group 11})$$

For group 10 metals, the $6a_{1g}$ and $5b_{1g}$ orbitals are involved in σ donation, the $2b_{2g}$ and $2e_g$ orbitals are involved in π back-donation, and the $7a_{1g}$ orbital is nonbonding, as shown in Figure 2b. For group 11 metals, as shown in Figure 2a, the $7t_2$ orbitals are involved in σ donation and the $8t_2$ orbitals are a little involved in π back-donation. Group 10 metal tetracarbonyl cations in the T_d structure are not stable because of the Jahn−Teller distortion, which could arise because the three degenerate $8t_2$ orbitals are not fully occupied. In the molecular orbital diagrams, it was clearly seen that the amount of σ donation is much larger than that of π back-donation for all group 10 and group 11 metal carbonyl cations, which will be discussed in the next subsection.

B. Dissociation Energies and M−C Bond Lengths. The dissociation energies for the loss of one carbonyl, D_0 (CO)s, were calculated using the following dissociation reaction:

$$[M(CO)_n]^{x+} \rightarrow [M(CO)_{n-1}]^{x+} + CO$$

Table 1 shows the D_0 (CO)s for group 10 and group 11 metal carbonyl cations, $[M(CO)_n]^{x+}$, given by the B3LYP and CCSD(T) methods, where the CCSD(T)//B3LYP values were calcu-

TABLE 1: Dissociation Energies for Loss of One Carbonyl D_0 (CO) (kcal/mol) of Group 10 $[M(CO)_n]^{2+}$ (M = Ni, Pd, Pt; n = 1−4) and Group 11 $[M(CO)_n]^{+}$ (M = Cu, Ag, Au; n = 1−4) Metal Carbonyl Cations

		D_0 (kcal/mol)[a]				D_0 (kcal/mol)[a]		
group 10	SYM	B3LYP	CCSD(T)//B3LYP	group 11	SYM	B3LYP	CCSD(T)//B3LYP	exp[b]
$[Ni(CO)]^{2+}$	$C_{\infty v}$	109.4	92.6	$[Cu(CO)]^{+}$	$C_{\infty v}$	38.5	36.7	36
$[Pd(CO)]^{2+}$	$C_{\infty v}$	130.4	111.4	$[Ag(CO)]^{+}$	$C_{\infty v}$	23.7	22.3	21
$[Pt(CO)]^{2+}$	$C_{\infty v}$	139.8	123.2	$[Au(CO)]^{+}$	$C_{\infty v}$	45.5	42.9	45
$[Ni(CO)_2]^{2+}$	$D_{\infty h}$	71.4	69.6	$[Cu(CO)_2]^{+}$	$D_{\infty h}$	37.5	39.1	41
	C_{2v}	72.1	69.7					
$[Pd(CO)_2]^{2+}$	$D_{\infty h}$	67.7	64.8	$[Ag(CO)_2]^{+}$	$D_{\infty h}$	25.6	26.0	26
	C_{2v}	71.7	69.4					
$[Pt(CO)_2]^{2+}$	$D_{\infty h}$	74.1	73.5	$[Au(CO)_2]^{+}$	$D_{\infty h}$	45.5	47.4	
	C_{2v}	88.5	86.7					
$[Ni(CO)_3]^{2+}$	C_{2v}	60.7	61.5	$[Cu(CO)_3]^{+}$	D_{3h}	15.5	17.2	18
$[Pd(CO)_3]^{2+}$	C_{2v}	58.6	59.3	$[Ag(CO)_3]^{+}$	D_{3h}	9.7	11.7	13
$[Pt(CO)_3]^{2+}$	C_{2v}	67.7	71.0	$[Au(CO)_3]^{+}$	D_{3h}	3.1	8.0	
$[Ni(CO)_4]^{2+}$	D_{4h}	54.9	57.6	$[Cu(CO)_4]^{+}$	T_d	13.3	15.9	13
$[Pd(CO)_4]^{2+}$	D_{4h}	53.9	56.7	$[Ag(CO)_4]^{+}$	T_d	6.8	7.1	11
$[Pt(CO)_4]^{2+}$	D_{4h}	63.4	68.0	$[Au(CO)_4]^{+}$	T_d	2.0	8.2	

[a] The corrections of BSSE and ZPE were done for D_0 (CO). [b] Gas phase experimental data for group 11 complexes are taken from ref 29.

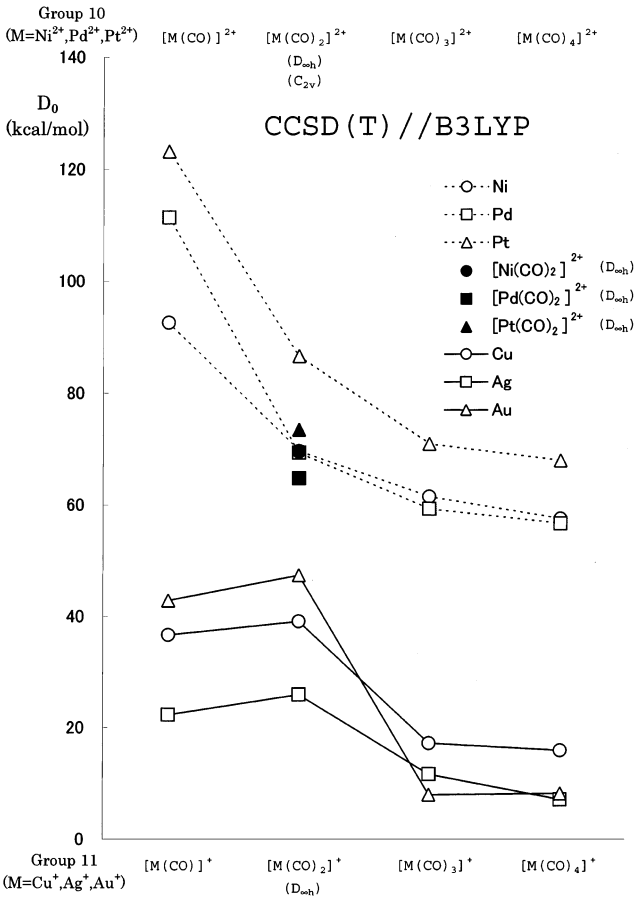

Figure 3. Dissociation energies (kcal/mol) for the loss of one carbonyl D_0(CO)s for $[M(CO)_n]^{x+}$ calculated by the CCSD(T)//B3LYP method. The dotted and solid lines show the results for group 10 and 11 metal complexes, respectively.

lated at the B3LYP optimized geometries. The BSSE and ZPE corrections were made for all of the D_0 (CO) values. The D_0 (CO)s of group 11 metal carbonyl cations are in good agreement with gas phase experimental data,[25] while no experimental data are available for group 10 metal complexes. Figure 3 illustrates the D_0 (CO)s obtained by CCSD(T)//B3LYP.

The D_0 (CO)s of group 10 metal carbonyl cations are much larger than those of group 11 metal carbonyl cations for all CO coordination numbers (n). For group 10 metals, the monocarbonyl cations are the most stable, the bent structure is more stable than the linear one for dicarbonyl cations, and the D_0 value decreases in going from di- to tetracarbonyl cations, while the change is very mild. For group 11 metals, the dicarbonyl cations are the most stable, and monocarbonyl cations are nearly as stable, while tri- and tetracarbonyl cations have very low stability.

Lipinetti et al. investigated systematically[16] the geometries and bond strengths of $[M(CO)_n]^{x+}$ (M^{x+} = Cu^+, Ag^+, Au^+, Zn^{2+}, Cd^{2+}, Hg^{2+}; n = 1−6). Because they are isoelectric complexes, group 12 complexes have the same molecular symmetries as the corresponding group 11 complexes. Their results for group 11 metal carbonyl cations are essentially the same as the present ones. Because the electrostatic effects are essential for the bonding in metal carbonyl cations, the D_0 (CO)s of doubly charged group 12 metal complexes are much larger than those of singly charged group 11 metal complexes for all CO coordination numbers (n). This is also the case for the doubly charged group 10 metal complexes treated in the present work.

Table 2 shows the R (M−C) values of group 10 and group 11 metal carbonyl cations. For group 10 metal complexes, R (M−C) shows very mild dependency on the kind of metal atom and also on the coordination number (n); the R (M−C)s are in the range of 1.89−2.05 Å. On the other hand, for group 11 metals complexes R (M−C) is very much dependent on the kind of metal atom and also on n; the R (M−C)s lengthen significantly from n = 2 to 3 and 4, especially for M = Ag and Au, and are in the range of 1.88−2.30 Å. Note that R (Pd−C) is nearly the same as R (Pt−C), while R (Ag−C) is longer than R (Au−C) by more than 0.1 Å. The reason is that the relativistic contraction of Au^+ is much larger than that of Pt^{2+}. These trends in R (M−C)s are roughly reflected in the trend in the D_0 (CO)s (see Figure 3 or Table 1).

Coulombic M^{x+}−CO interactions become more significant than the covalent interactions for the M−C bonds of doubly charged metal complexes.[16] However, with reference to the amounts of the σ donation and π back-donation, we can discuss the differences in D_0 (CO)s among $[M(CO)_n]^{x+}$ for a given cationic charge. The cationic metal promotes the σ donation from CO(5σ) to metal, while it reduces the π back-donation from metal to CO($2\pi^*$), as compared to the neutral metal. Both σ donation and π back-donation contribute to strengthen the covalent M−C bonds. Figure 4 illustrates the amounts of σ donation and π back-donation per carbonyl for $[M(CO)_n]^{x+}$ obtained by Mulliken population analysis based on the B3LYP

TABLE 2: Optimized Geometries of Group 10 $[M(CO)_n]^{2+}$ (M = Ni, Pd, Pt; n = 1, 2, 4) and Group 11 $[M(CO)_n]^{+}$ (M = Cu, Ag, Au; n = 1−4) Metal Carbonyl Cations, Obtained by the B3LYP Method

group 10	SYM	R (M−C) (Å)	R (C−O) (Å)[a]	θ (C−M−C) (°)	group 11	SYM	R (M−C) (Å)	R (C−O) (Å)[a]
				monocarbonyl cations				
$[Ni(CO)]^{2+}$	$C_{\infty v}$	1.906	1.107 (−0.019)		$[Cu(CO)]^{+}$	$C_{\infty v}$	1.881	1.115 (−0.011)
$[Pd(CO)]^{2+}$	$C_{\infty v}$	1.904	1.110 (−0.016)		$[Ag(CO)]^{+}$	$C_{\infty v}$	2.180	1.115 (−0.011)
$[Pt(CO)]^{2+}$	$C_{\infty v}$	1.893	1.111 (−0.015)		$[Au(CO)]^{+}$	$C_{\infty v}$	1.958	1.116 (−0.010)
				dicarbonyl cations				
$[Ni(CO)_2]^{2+}$	$D_{\infty h}$	1.969	1.108 (−0.018)	180.0	$[Cu(CO)_2]^{+}$	$D_{\infty h}$	1.906	1.115 (−0.011)
	C_{2v}	1.888	1.109 (−0.017)	92.2				
$[Pd(CO)_2]^{2+}$	$D_{\infty h}$	2.045	1.109 (−0.017)	180.0	$[Ag(CO)_2]^{+}$	$D_{\infty h}$	2.141	1.115 (−0.011)
	C_{2v}	1.945	1.111 (−0.015)	86.6				
$[Pt(CO)_2]^{2+}$	$D_{\infty h}$	2.035	1.110 (−0.016)	180.0	$[Au(CO)_2]^{+}$	$D_{\infty h}$	2.007	1.115 (−0.011)
	C_{2v}	1.905	1.113 (−0.013)	89.3				
				tricarbonyl cations				
$[Ni(CO)_3]^{2+}$	C_{2v}	1.870	1.111 (−0.015)		$[Cu(CO)_3]^{+}$	D_{3h}	1.958	1.117 (−0.009)
		1.941	1.110 (−0.016)					
$[Pd(CO)_3]^{2+}$	C_{2v}	1.947	1.112 (−0.014)		$[Ag(CO)_3]^{+}$	D_{3h}	2.231	1.117 (−0.009)
		2.044	(1.110) (−0.016)					
$[Pt(CO)_3]^{2+}$	C_{2v}	1.895 (−0.012)	1.114		$[Au(CO)_3]^{+}$	D_{3h}	2.100	1.118 (−0.008)
		2.028 (−0.015)	1.111					
				tetracarbonyl cations				
$[Ni(CO)_4]^{2+}$	D_{4h}	1.919	1.111 (−0.015)		$[Cu(CO)_4]^{+}$	T_d	2.000	1.118 (−0.008)
$[Pd(CO)_4]^{2+}$	D_{4h}	2.036	1.111 (−0.015)		$[Ag(CO)_4]^{+}$	T_d	2.298	1.118 (−0.008)
$[Pt(CO)_4]^{2+}$	D_{4h}	2.016	1.112 (−0.014)		$[Au(CO)_4]^{+}$	T_d	2.170	1.119 (−0.007)
free CO		B3LYP	1.126				exp	1.127

[a] The differences from free CO value obtained by the B3LYP method are given in parentheses.

results. The σ donation is much larger than the π back-donation for all group 10 and group 11 complexes. This is contrary to what is seen in neutral metal carbonyls, in which π back-donation predominates.[1] Group 10 metal dications gain a much larger σ donation than group 11 metal monocations. The σ donation for group 11 metal complexes (0.2−0.5e) is about half that of group 10 metal ones (0.5−0.9e). The amounts of σ donation and π back-donation are related to the atomic orbital energies of metals. Because metal cations decrease their positive charges by the σ donations, they are approximately M^+ and M^0 in group 10 and group 11 complexes, respectively. Figure 5a,b plots the valence orbital energies, ϵ_s and ϵ_d, of $M^{+4}F(d^8s^1)$ and $M^2D(d^{10}s^1)$ for group 10 and group 11 metals, respectively, given by Cowan and Griffin's quasi-relativistic Hartree−Fock (QRHF) method. The ϵ_d values of $M^{2+3}F(d^8)$ and $M^{+1}S(d^{10})$ for group 10 and group 11 metals, respectively, are also included in Figure 5 for comparison. The relativistic effects stabilize the s orbital energy ϵ_s and destabilize the d orbital energy ϵ_d, especially in the third row transition metal ions. For group 10 metals, the amount of π back-donation increases in the order Ni < Pd < Pt for all n = 1−4 as shown in Figure 4a, along with the increase in the ϵ_d values. The amount of σ donation is in the order Ni ≈ Pt <Pd, which is correlated with the ϵ_s values. As for the group 11 metals, both σ donation and π back-donation are smallest for M = Ag, which is essentially due to the long Ag−C distance in $[Ag(CO)_n]^+$ (see Table 2). The ϵ_d is lowest for M = Ag, which also reduces the π back-donation in $[Ag(CO)_n]^+$. From the above analysis, it is concluded that the contributions of σ donation and π back-donation in group 10 and group 11 metal carbonyl cations act in tandem with the relativistic effects in their metal ions.

We can find that the sums of the amounts of σ donation and π back-donation (see Figure 4a,b) are roughly correlated with the D_0 (CO) values in Figure 3. For group 10 metal complexes, both σ donation and π back-donation are stronger in the bent dicarbonyl cations $[M(CO)_2]^{2+}$ (C_{2v}) than in the linear ones $[M(CO)_2]^{2+}$ ($D_{\infty h}$) for all M = Ni, Pd, and Pt; accordingly, D_0 (CO)s of bent structures are larger than those of linear structures. Even for tetracarbonyl cations, the σ donations are larger than 0.5e for all M = Ni, Pd, and Pt, and thus, they have large D_0 (CO)s (>55 kcal/mol). The D_0 (CO)s are significantly reduced from n = 1−2, which is mainly due to the larger Coulombic M^{2+}−CO interaction in monocarbonyl cations than in dicarbonyl cations, because the positive charge at the metal ions in dicarbonyl cations is reduced by the σ donations from two carbonyls. Among the three metals, Ni, Pd, and Pt, D_0 (CC) is largest for $[Pt(CO)_n]^{2+}$ for all n = 1−4. This is mainly caused by the largest π back-donation for Pt complexes.

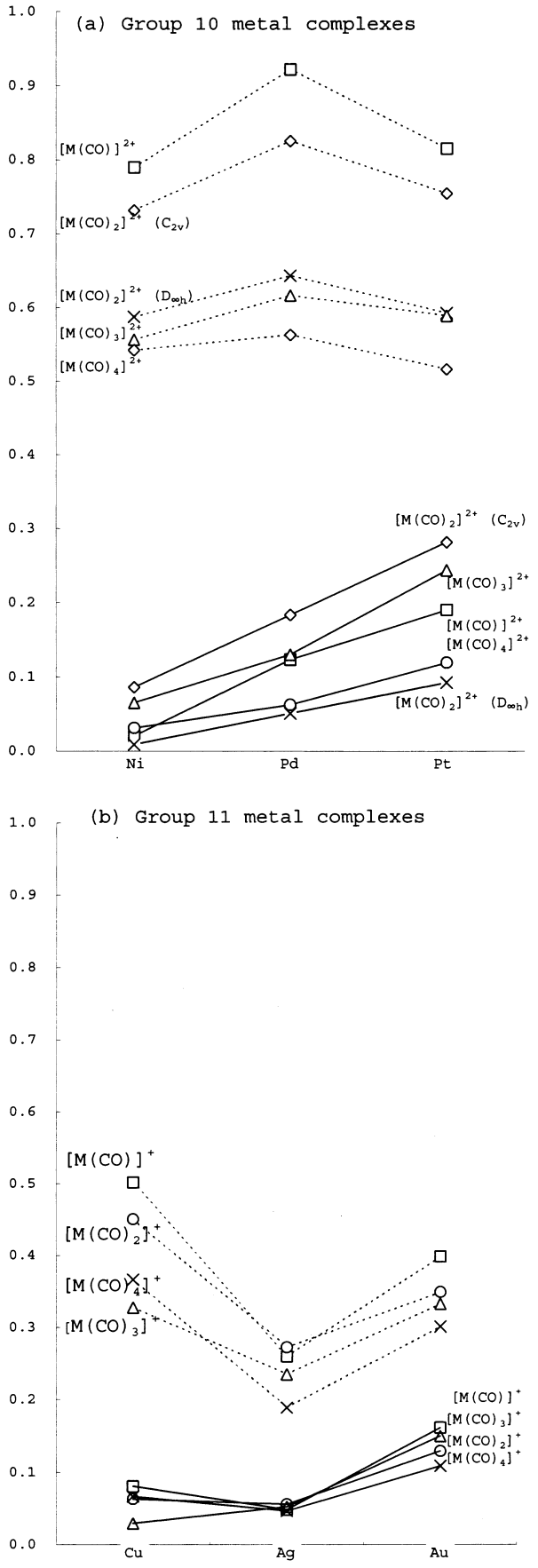

Figure 4. Amounts of s donation and p back-donation per carbonyl of (a) group 10 and (b) group 11 metal carbonyl cations given by Mulliken population analysis based on the B3LYP results.

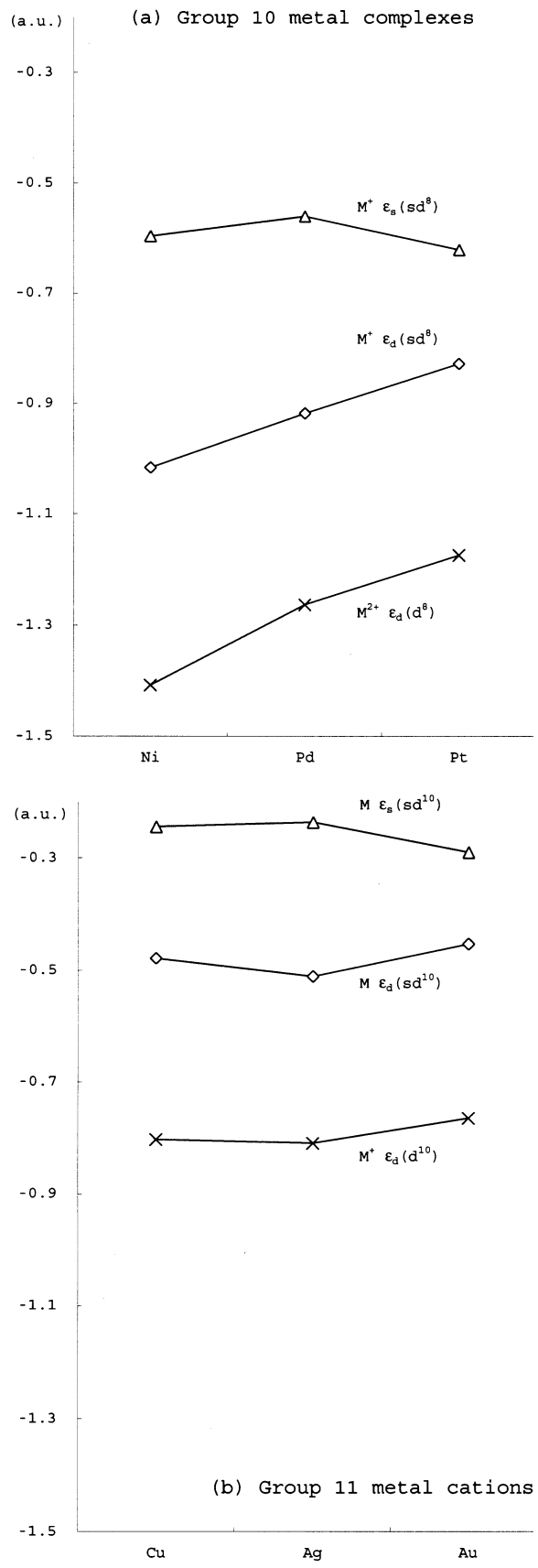

Figure 5. Valence orbital energies (au), e_s and e_d, (a) for $M^{+4}F(d^8s^1)$ and $M^{2+3}F(d^8)$ for group 10 metals and (b) for $M^{+1}S(d^{10})$ and $M^2D(d^{10}s^1)$ for group 11 metals, obtained by Cowan and Griffin's quasi-relativistic Hartree−Fock method.

TABLE 3: Vibrational Frequencies ν(CO) (cm^{-1}) for Group 10 $[M(CO)_n]^{2+}$ (M = Ni, Pd, Pt; n = 1, 2, 4) Metal Carbonyl Cations, Obtained by the B3LYP Method[a,b]

$[M(CO)]^{2+}$		$[M(CO)_2]^{2+}$			$[M(CO)_3]^{2+}$			$[M(CO)_4]^{2+}$			
	ν(CO) (cm^{-1})		ν(CO) (cm^{-1})			ν(CO) (cm^{-1})			ν(CO) (cm^{-1})		
SYM	IR	SYM	IR	Raman	SYM	IR		SYM	IR		
	$[Ni(CO)]^{2+}$		$[Ni(CO)_2]^{2+}$			$[Ni(CO)_3]^{2+}$			$[Ni(CO)_4]^{2+}$		
$C_{\infty v}$	Σ^+	$D_{\infty h}$	Σ_u	Σ_g	C_{2v}	B_2	A_1	D_{4h}	E_u	B_{1g}	A_g
	2309		2304	2308		2287	2289		2267	2274	2282
	(166)		(161)	(165)		(144)	(146)		(124)	(131)	(139)
		C_{2v}	B_2	A_1							
			2287	2289							
			(144)	(146)							
	$[Pd(CO)]^{2+}$		$[Pd(CO)_2]^{2+}$			$[Pd(CO)_3]^{2+}$			$[Pd(CO)_4]^{2+}$		
$C_{\infty v}$	Σ^+	$D_{\infty h}$	Σ_u	Σ_g	C_{2v}	B_2	A_1	D_{4h}	E_u	B_{1g}	A_g
	2273		2278	2294		2257	2277		2262	2271	2288
	(130)		(135)	(151)		(114)	(134)		(119)	(128)	(145)
		C_{2v}	B_2	A_1							
			2258	2278							
			(115)	(135)							
	$[Pt(CO)]^{2+}$		$[Pt(CO)_2]^{2+}$			$[Pt(CO)_3]^{2+}$			$[Pt(CO)_4]^{2+}$		
$C_{\infty v}$	Σ^+	$D_{\infty h}$	Σ_u	Σ_g	C_{2v}	B_2	A_1	D_{4h}	E_u	B_{1g}	A_g
	2267		2270	2296		2243	2271		2251	2270	2293
	(124)		(127)	(153)		(100)	(128)		(108)	(127)	(150)
		C_{2v}	B_2	A_1							
			2245	2272							
			(102)	(129)							

[a] The ν(CO) values were factorized by 0.9690, which is a ratio of $\nu(CO)_{exp}$ = 2143 cm^{-1} to $\nu(CO)_{B3LYP}$ for free CO; see text for details. [b] The differences from free CO value are given in parentheses.

TABLE 4: Vibrational Frequencies ν(CO) (cm^{-1}) for Group 11 $[M(CO)_n]^+$ (M = Cu, Ag, Au; n = 1−4) Metal Carbonyl Cations, Obtained by the B3LYP Method[a,b]

$[M(CO)]^+$		$[M(CO)_2]^+$			$[M(CO)_3]^+$			$[M(CO)_4]^+$		
	ν(CO) (cm^{-1})		ν(CO) (cm^{-1})			ν(CO) (cm^{-1})			ν(CO) (cm^{-1})	
SYM	IR	SYM	IR	Raman	SYM	IR	Raman	SYM	IR	Raman
	$[Cu(CO)]^+$		$[Cu(CO)_2]^+$			$[Cu(CO)_3]^+$			$[Cu(CO)_4]^+$	
$C_{\infty v}$	Σ^+	$D_{\infty h}$	Σ_u+	Σ_g+	D_{3h}	E′	A$_1$′	T_d	T_2	A_1
	2240		2228	2253		2207	2230		2198	2221
	(97)		(85)	(110)		(64)	(87)		(55)	(78)
	2234[c]		2230[c]			2211[c]			2202[c]	
	$[Ag(CO)]^+$		$[Ag(CO)_2]^+$			$[Ag(CO)_3]^+$			$[Ag(CO)_4]^+$	
$C_{\infty v}$	Σ^+	$D_{\infty h}$	Σ_u	Σ_g	D_{3h}	E′	A$_1$′	T_d	T_2	A_1
	2238		2232	2243		2213	2222		2204	2213
	(95)		(89)	(100)		(70)	(79)		(61)	(70)
	2235[d]		2233[d]			2216[d]			2206[d]	
	$[Au(CO)]^+$		$[Au(CO)_2]^+$			$[Au(CO)_3]^+$			$[Au(CO)_4]^+$	
$C_{\infty v}$	Σ^+	$D_{\infty h}$	Σ_u	Σ_g	D_{3h}	E′	A$_1$′	T_d	T_2	A_1
	2233		2226	2259		2196	2217		2187	2208
	(90)		(83)	(116)		(53)	(74)		(44)	(65)
	2237[d]		2234[d]			2203[d]			2194[d]	

[a] The ν(CO) values were factorized by 0.9690, which is a ratio of $\nu(CO)_{exp}$ = 2143 cm^{-1} to $\nu(CO)_{B3LYP}$ = 2211 cm^{-1} for free CO; see text for details. [b] The differences from free CO value are given in parentheses. [c] Experimental data taken from ref 13. [d] Experimental data taken from ref 14.

For group 11 metal complexes, the amounts of both σ donation and π back-donation are smallest for M = Ag as shown in Figure 4b, resulting in $[Ag(CO)_n]^+$ having the smallest D_0 (CO) for n = 1, 2, and 4. D_0 (CO) is the largest for $[Au(CO)_n]^+$ for n = 1 and 2. The largest amount of π back-donation for M = Au (Figure 4b) contributes to strengthen the Au−C bond. The dicarbonyl cations have slightly larger D_0 (CO)s than the monocarbonyl cations. The rather high bond energies of mono- and dicarbonyl cations have been attributed to a favorable s−d$_\sigma$ hybridization, which removes metal−ion electron density from the bonding axis and thereby enhances charge donation from σ-donor ligands.[16,18] Because a majority of the energy cost for the hybridization is paid during the formation of the first M^+−CO bond, the second D_0 (CO) value is higher than the first.[16] The loss of the s−d$_\sigma$ hybridization reduces the stability of tri- and tetracarbonyl cations. The positive charge at the metal ion decreases with the increase of the number of ligands, which leads to weaker Coulombic attractions. In addition, the ligand−ligand repulsion grows with the number of ligands. Thus, D_0 (CO) values are significantly reduced from n = 2 to 3 and 4 for group 11 complexes. The charge−dipole bonding is linear in the charge, the charge-induced dipole term is quadratic in the charge, and the elimination of one electron will reduce the metal−ligand repulsion. Thus, the group 10 dicationic complexes should be much more strongly bound than the group 11 monocationic complexes.

C. CO Vibrational Frequencies and C−O Bond Lengths. The CO vibrational frequencies ν(CO) of $[M(CO)_n]^{x+}$ are given in Tables 3 and 4 for M = group 10 and group 11 metals, respectively. Experimental data of infrared spectra (IR) for group 11 metal complexes[13,14] are also included in Table 4. All of the ν(CO)s are higher than that of free CO (2143 cm^{-1}); accord-

ingly, the R (C−O)s in Table 2 are shorter than that of free CO (1.126 Å, B3LYP). On the basis of a detailed analysis, Goldman and Jespersen[17] concluded that electrostatic effects contribute essentially to an increase in the ν(CO)s of carbonyl cations and the π back-donation induces a decrease in the values, while the σ donation does not contribute to the change in the ν(CO)s because the 5σ orbital is essentially nonbonding. The ν(CO)s of doubly charged group 10 metal complexes are higher than those of free CO by 100−165 cm^{-1}, while those of singly charged group 11 metal complexes are higher by 50−110 cm^{-1}. The higher ν(CO) of the group 10 metal complexes indicates that the electrostatic effects on the CO bonds are much stronger than the effects of π back-donation; the amounts of π back-donation are even larger for M = group 10 (Figure 4a) than for M = group 11 (Figure 4b). The R (C−O)s are shortened by 0.015−0.020 Å for group 10 metal complexes and by 0.007−0.011 Å for group 11 metal complexes. The changes in R (C−O) are in accord with the changes in ν(CO)s.

Although the electrostatic effects dominate to strengthen the C−O bonds, when we compare the ν(CO)s of group 10 and group 11 complexes separately, it is found that the amount of π back-donation correlates well with the ν(CO) values. The amount of π back-donation in Figure 4a is larger for $[M(CO)_2]^{2+}$ in the C_{2v} structure than in the $D_{\infty h}$ structure for each of M = Ni, Pd, and Pt, and thus, the former has a lower ν(CO) than the latter. The amount of π back-donation increases in the order Ni < Pd < Pt, as shown in Figure 4a, which correlates well with the corresponding order in the ν(CO) values in Table 3; for a given n, ν(CO) decreases in the order Ni > Pd > Pt for each mode of $[M(CO)_n]^{2+}$. For group 11 metal complexes, the correlation is not so clear; however, for a given n, the largest π back-donation arises for the M = Au complexes, leading to the lowest ν(CO) of $[Au(CO)_n]^+$. The calculated ν(CO)s agree well with the observed IR values for group 11 metal complexes[13,14] in Table 4.

4. Conclusions

In this paper, the electronic structures of group 10 and group 11 metal carbonyl cations, $[M(CO)_n]^{x+}$ ($M^{x+} = Ni^{2+}$, Pd^{2+}, Pt^{2+}, Cu^+, Ag^+, Au^+; $n = 1-4$), were investigated using density functional methods (B3LYP) and coupled cluster methods (CCSD(T)). Group 11 metal mono-, di-, tri-, and tetracarbonyl cations have their energy minimum in the $C_{\infty v}$, $D_{\infty h}$, D_{3h}, and T_d structures, respectively. Because the number of valence electrons of group 10 metal complexes is two less than in the corresponding group 11 metal complexes, the geometrical structures differ. Group 10 metal dicarbonyl cations have the $D_{\infty h}$ and C_{2v} structures, and the complexes are more stable in the C_{2v} structure than in the $D_{\infty h}$ structure. Tri- and tetracarbonyl cations have T-shaped (C_{2v}) and D_{4h} structures, respectively. These optimized structures are in good agreement with the available experimental ones.[3,4,19]

The binding energies D_0 (CO) given by B3LYP and CCSD(T)//B3LYP after BSSE and ZPE corrections are in good agreement with available experimental data. The D_0 (CO)s of group 10 metal complexes are much larger than those of group 11 metal complexes. For group 10 metal complexes, D_0 (CO) decreases significantly from $n = 1-2$, while the change is mild from $n = 2-4$. Group 10 metal tetracarbonyl cations still have large D_0 (CO)s (>55 kcal/mol). D_0 (CO)s of group 11 complexes decrease significantly from $n = 2-3$. These trends in D_0 (CO)s can be explained by the nature of the M^{x+}−CO bonding interactions. Coulombic interactions are dominant for the bonding, while covalent interactions through σ donation and a little π back-donation enhance the bonding. Both Coulombic and covalent interactions are larger in group 10 dicationic complexes than in group 11 monocationic complexes. Because the positive charge at the metal ion decreases with the increase of the number of ligands, D_0 (CO) tends to decrease in going from $n = 1-4$. Exceptionally, for group 11, dicarbonyl cations have slightly larger D_0 (CO) than monocarbonyl cations, which is caused by the $s-d_\sigma$ hybridization at the metal ion.

The third row metal complexes, $M^{2+} = Pt^{2+}$ and $M^+ = Au^+$, tend to have the largest D_0 (CO) among group 10 and group 11 complexes. This is explained by the fact that the relativistic contraction of the M^{x+} radius is larger for the third row metal ions than for the second row metal ions. Both electrostatic and covalent contributions favor the shorter M−C bond. In addition, the valence d orbitals of the third row metal ions are largely destabilized by relativistic effects, resulting in a larger amount of π back-donation, which contributes to strengthening the M−C bonds and weakening the C−O bonds.

All of the ν(CO)s are higher than those of free CO (2143 cm^{-1}). The ν(CO)s of doubly charged group 10 metal complexes are higher than those of free CO by 100−165 cm^{-1}, while those of singly charged group 11 metal complexes are higher by 50−110 cm^{-1}. Although electrostatic contributions are essential for strengthening the C−O bonds, the π back-donation contributes visibly to weakening the C−O bonds. For a given n, the ν(CO) of group 10 complexes tends to decrease in the order M = Ni > Pd > Pt, which correlates well with the increase in π back-donation, M = Ni < Pd < Pt. The correlation is not clear for group 11 metal complexes; however, for a given n, the largest π back-donation arises for the M = Au complexes, leading to the lowest ν(CO) of $[Au(CO)_n]^+$.

The group 11 metal dicarbonyl cations are catalysts for the Koch reaction,[8−10] while there is no report of a reaction catalyzed by group 10 metal carbonyl cations. The high reactivity of metal carbonyl cations in the Koch reaction comes from the much higher stability of the dicarbonyl cation than the tri- and tetracarbonyl cations for group 11 complexes. The dicarbonyl cation could form complexes for alkylation by the Koch reaction, instead of making unstable tri- or tetracarbonyl complexes. We will study the reaction mechanism of the catalytic carbonylation reactions of olefins with group 11 metal carbonyl cations in our next paper.

Acknowledgment. This research was supported by a Grant-in-Aid for Scientific Research from the Ministry of Education, Science, and Culture of Japan. We thank the Computer Center of the Institute for Molecular Science for the use of the Fujitsu VPP5000, SGI 2800, NEC SX-5, HPC, and IBM SP2 computers.

References and Notes

(1) For reviews, see (a) Colquhoum, H. M.; Thompson, D. J.; Twigg, M. V. *Carbonylation: Direct Synthesis of Carbonyl Compounds*; Plenum Press: New York, 1991. (b) Henrici-Olivé, G.; Olivé, S. *The Chemistry of the Catalyzed Hydrogenation of Carbon Monoxide*; Springer: Berlin, 1983.

(2) (a) Souma, Y.; Sano, H. *J. Org. Chem.* **1973**, *38*, 3633. (b) Souma, Y.; Sano, H. *Bull. Chem. Soc. Jpn.* **1974**, *47*, 1717. (c) Souma, Y.; Iyoda, J.; Sano, H. *Inorg. Chem.* **1976**, *15*, 968.

(3) Rock, J. J.; Strauss, S. H. *Catal. Today* **1997**, *36*, 99.

(4) (a) Willner, H.; Aubke, F. *Inorg. Chem.* **1990**, *29*, 2195. (b) Willner, H.; Schaebs, S.; Hwang, G.; Mistry, F.; Jones, R.; Trotter, J.; Aubke, F. *J. Am. Chem. Soc.* **1992**, *114*, 8972.

(5) Xu, Q.; Souma, Y. *Top. Catal.* **1998**, *6*, 17.

(6) Ivanova, S. M.; Ivanov, S. V.; Miller, S. M.; Anderson, O. P.; Solntsev, K. A.; Strauss, S. H. *Inorg. Chem.* **1999**, *38*, 3756.

(7) Hurlburt, P. K.; Rack, J. J.; Luck, J. S.; Dec, S. F.; Webb, J. D.; Anderson, O. P.; Strauss, S. H. *J. Am. Chem. Soc.* **1994**, *116*, 10003.

(8) Koch, H. *Brennst. Chem.* **1955**, *36*, 321.

(9) Xu, Q.; Imamura, Y.; Fujiwara, M.; Souma, Y. *J. Org. Chem.* **1997**, *36*, 158.

(10) (a) Souma, Y.; Sano, H.; Miwa, H.; Kawasaki, H.; Ichikawa, O. *J. Synth. Org. Chem.* **1990**, *48*, 92. (b) Souma, Y.; Kawasaki, H. *Catal. Today* **1997**, *36*, 91.

(11) Barnes, L. A.; Rosi, M.; Bauschlicher, C. W. *J. Chem. Phys.* **1991**, *94*, 2031.

(12) Lupinetti, A. J.; Jonas, V.; Thiel, W.; Strauss, S. H.; Frenking, G. *Chem. Eur. J.* **1999**, *5* (9), 2573.

(13) Goldman, A. S.; Krogh-Jespersen, K. *J. Am. Chem. Soc.* **1996**, *118*, 12159.

(14) Lupinetti, A. J.; Frenking, G.; Strauss, S. H. *J. Phys. Chem.* **1997**, *101*, 9551.

(15) (a) Calderazzo, F.; Belli, D. D. *Inorg. Chem.* **1981**, *20*, 1310. (b) Wang, C.; Willner, H.; Bodenbinder, M.; Batchelor, R. J.; Einstein, F. W. B.; Aubke, F. *Inorg. Chem.* **1994**, *33*, 3521. (c) Hwang, G.; Wang, C.; Bodenbinder, M.; Willner, H.; Aubke, F. *J. Fluorine Chem.* **1994**, *66*, 159. (d) Hwang, G.; Wang, C.; Aubke, F.; Willner, H.; Bodenbinder, M. *Can. J. Chem.* **1993**, *71*, 1532. (e) Uson, R.; Froniès, J.; Tomàs, M.; Menjon, B. *Organometallics* **1985**, *4*, 1912. (f) Andreini, B. P.; Belli, D. D.; Calderazzo, F.; Venturi, M. G.; Pilizzi, G.; Segre, A. *J. Organomet. Chem.* **1988**, *354*, 357.

(16) Xu, Q.; Heaton, B. T.; Jacob, C.; Mogi, K.; Ichihashi, Y.; Souma, Y.; Kanamori, K.; Eguchi, T. *J. Am. Chem. Soc.* **2000**, *122*, 6862.

(17) Mogi, K.; Sakai, Y.; Sonoda, T.; Xu, Q.; Souma, Y. *J. Mol. Struct. (THEOCHEM)* **2001**, *537*, 125.

(18) Becke, A. D. *J. Chem. Phys.* **1993**, *98*, 5648.

(19) Parr, R. G.; Yang, W. *Density-Functional Theory of Atoms and Molecules*; Oxford University Press: New York, 1989.

(20) (a) Cizek. *Adv. Chem. Phys.* **1969**, *14*, 35. (b) Taylor, P. R. In *Lecture Notes in Quantum Chemistry II*; Roos, B. O., Ed.; Springer: Berlin, 1994. (c) Lee, T. J.; Scuseria, G. E. In *Quantum Mechanical Electronic Structure Calculations with Chemical Accuracy*; Langhoff, S. R., Ed.; Kluwer: Dordrecht, 1995. (d) Bartlett, R. J.; Stanton, J. F. In *Review in Computation Chemistry*; Lipkowitz, K. B., Boyd, D. B., Eds.; VCH: New York, 1994; Vol. 5.

(21) (a) Stevens, W. J.; Basch, H.; Krauss, M. *J. Chem. Phys.* **1984**, *81*, 6026. (b) Stevens, W. J.; Cundari, T. R.; Stevens, W. J. *J. Chem. Phys.* **1993**, *98*, 5555.

(22) Woon, E.; Dunning, T. H., Jr. *J. Chem. Phys.* **1993**, *98*, 1358.

(23) Dargel, T. K.; Hertwig, R. H.; Koch, W.; Horn, H. *J. Chem. Phys.* **1998**, *108*, 3876.

(24) Frisch, M. J.; Trucks, G. W.; Schlegel, H. B.; Scuseria, G. E.; Robb, M. A.; Cheeseman, J. R.; Zakrzewski, V. G.; Montgomery, J. A., Jr.; Stratmann, R. E.; Burant, J. C.; Dapprich, S.; Millam, J. M.; Daniels, A. D.; Kudin, K. N.; Strain, M. C.; Farkas, O.; Tomasi, J.; Barone, V.; Cossi, M.; Cammi, R.; Mennucci, B.; Pomelli, C.; Adamo, C.; Clifford, S.; Ochterski, J.; Petersson, G. A.; Ayala, P. Y.; Cui, Q.; Morokuma, K.; Malick, D. K.; Rabuck, A. D.; Raghavachari, K.; Foresman, J. B.; Cioslowski, J.; Ortiz, J. V.; Stefanov, B. B.; Liu, G.; Liashenko, A.; Piskorz, P.; Komaromi, I.; Gomperts, R.; Martin, R. L.; Fox, D. J.; Keith, T.; Al-Laham, M. A.; Peng, C. Y.; Nanayakkara, A.; Gonzalez, C.; Challacombe, M.; Gill, P. M. W.; Johnson, B. G.; Chen, W.; Wong, M. W.; Andres, J. L.; Head-Gordon, M.; Replogle, E. S.; Pople, J. A. *Gaussian 98*, revision A.5; Gaussian, Inc.: Pittsburgh, PA, 1998.

(25) Meyer, F.; Chen, Y. M.; Armentrout, P. B. *J. Am. Chem. Soc.* **1995**, *117*, 4071.